Refractive index dependence of the transmission properties for a photonic crystal array of dielectric spheres

T. Kondo*
Institute of Industrial Science, University of Tokyo, 4-6-1 Komaba, Meguroku, Tokyo 153-8505, Japan

S. Yamaguti
Graduate School of Science and Technology, Chiba University, 1-33 Yayoicho, Inageku, Chiba 263-8522, Japan

M. Hangyo
Laser Terahertz Division, Institute of Laser Engineering, Osaka University, 2-6 Yamadaoka, Suita, Osaka 565-0871, Japan

K. Yamamoto† and Y. Segawa
Photodynamics Research Center, The Institute of Physical and Chemical Research (RIKEN), 519-1399 Aoba, Aramaki, Aobaku, Sendai 980-0845, Japan

K. Ohtaka
Center for Frontier Science, Chiba University, 1-33 Yayoicho, Inageku, Chiba 263-8522, Japan
(Received 21 September 2004; published 8 December 2004)

The refractive index dependence of the transmission properties for a two-dimensional photonic crystal array of dielectric spheres has been investigated. The transmission properties of a Si_3N_4 ($n \sim 2.99$) sphere-array photonic crystal and a polytetrafluoroethylene (PTFE, $n \sim 1.44$) sphere-array photonic crystal are measured in the sub-THz frequency region. The experimental photonic band structures show good agreement with those calculated by the vector Korringa-Kohn-Rostoker method. They are also compared with the optical density of states of the gallery mode localized in an isolated sphere and the photonic band structure based on the guided wave mode in a dielectric slab. The results indicate that the characteristics of the gallery mode appear in the photonic band structure of the Si_3N_4 sphere-array photonic crystal. On the other hand, the characteristics of the guided wave mode appear dominantly in the photonic band structure of the PTFE sphere-array photonic crystal. The crossover from the guided-wave-like to the localized-gallery-mode-like characteristics occurs with increasing refractive index of the material.

DOI: 10.1103/PhysRevB.70.235113 PACS number(s): 42.70.Qs, 78.47.+p, 42.25.Bs

I. INTRODUCTION

Photonic crystals,[1–3] which are artificial structures with periodic modulation of the refractive index, have been extensively studied for various applications such as lasing,[4] waveguides,[5] high-Q nanocavities,[6] etc. The physics of the photonic crystal is based on the interaction between the photonic crystal and an electromagnetic wave. The phenomenon of electromagnetic wave confinement in a photonic crystal is one of the most valuable properties for such applications, and its characteristics are determined by the structures and optical properties of the mother materials.

The design of structures for photonic crystals is one of the important processes for realizing strong confinement of the electromagnetic wave. An array of dielectric spheres is one of the candidates for such structures because of the extremely strong confinement associated with the "gallery mode" of the individual spheres. The incident electromagnetic wave in each isolated dielectric sphere undergoes an attractive potential and suffers Mie scattering. In a sphere-array photonic crystal, the electromagnetic wave confined by multiscattering within the sphere can hop from one sphere to its neighbor through optical tunneling. The coherent hopping motion of the electromagnetic wave in a sphere-array photonic crystal gives rise to a photonic band. Therefore, the photonic band in a sphere-array photonic crystal reflects the original character of the confinement effect of the gallery modes.[7]

The degree of optical confinement increases with increasing refractive index of the material because a larger refractive index of the material induces a stronger attractive potential for the electromagnetic wave. However, the relation between the optical properties of the photonic crystal and the refractive index of the material has not been discussed systematically. This is because it is difficult to prepare samples with sufficient accuracy in the visible and near-infrared regions.

Recently, the authors have demonstrated that good agreement between experiments and theoretical calculations is obtained for a two-dimensional (2D) Si_3N_4 sphere-array photonic crystal in the sub-THz region.[7,8] In particular, it was pointed out that incorporating the absorption by the constituent material is essential for complete agreement between the experiment and theory.[8] Very recently, Smith-Purcell radiation using a 2D sphere-array photonic crystal was predicted[9] and demonstrated experimentally.[10] The sub-THz and THz regions are suitable for elucidating the basic properties of photonic crystals because samples with reasonable size and accuracy can be fabricated without significant

difficulty.[7,8,10–13] In this work, we investigated the refractive index dependence of the transmission properties for dielectric-sphere-array photonic crystals in the sub-THz region. Two sphere-array photonic crystals, the materials of which are Si_3N_4 ($n \sim 2.99$) and polytetrafluoroethylene (PTFE, $n \sim 1.44$), were prepared. The transmission properties were measured using THz time domain spectroscopy (THz TDS).[14,15] The transmission spectra are compared with an accurate calculation based on the vector Korringa-Kohn-Rostoker (KKR) method.[1,16] The experimental results were also compared with the optical density of states (ODOS) of the gallery modes for an isolated dielectric sphere and the photonic band structure based on the guided wave mode in a dielectric slab.

II. EXPERIMENT

2D arrays of dielectric spherical balls with diameter $d = 3.175$ mm were prepared and investigated. We used Si_3N_4 and PTFE spheres in this study. In advance, the dispersion relation of the complex refractive indices $n - i\kappa$ of these bulk materials was measured by THz TDS.[14,15] The results indicate that the complex refractive index of Si_3N_4 shows a weak dispersion relation, for example, $2.962 - 0.0043i$ at 50 GHz and $2.992 - 0.0054i$ at 100 GHz,[8] whereas that of PTFE shows a nearly constant value of $1.437 - 0.0002i$ in the frequency region examined. The Si_3N_4 and PTFE spheres are guaranteed to have a highly perfect spherical shape and quite uniform size with a variation in diameter of less than 0.05 mm ($<1\%$). These spheres were manually placed in a monolayer triangular lattice with a lattice constant $a = d$, corresponding to a situation where the spheres touch each other, in an aluminum frame. The sample sizes of the Si_3N_4 and PTFE sphere arrays are 42×50 mm^2 and 50×75 mm,[2] respectively. One face of the resulting photonic crystals was fixed by a 55-μm-thick vinyl film, the transmittance of which is 93% in the sub-THz frequency region.

The transmission characteristics of the sample were measured using THz TDS in the atmosphere. The incident beam was a *p*-polarized THz wave transmitted through an aperture of diameter less than 40 mm, which is smaller than the size of the sample. (The area outside the sample was covered with the aluminum frame.) Since the illuminated area contains about 200 spheres, the finite-size effect is neglected. The 2D wave vector of the incident wave along the sample surface is set along the symmetry axis Γ-M of the 2D Brillouin zone. The zeroth-order power transmission spectra were obtained from the THz wave forms in the time domain. Details about the experimental setup are described in a previous paper.[8]

III. RESULTS AND DISCUSSION

Figure 1 shows the time domain electromagnetic wave forms of the incident THz wave and the THz waves transmitted through the sphere array at normal incidence. Since the optical length is proportional to the refractive index of the material, the THz wave transmitted through the Si_3N_4 sphere array arrives at the detector much later than that transmitted through the PTFE sphere array. Figure 1(b) shows that an oscillating wave form, which is different from the reference wave form, appears in the THz wave transmitted through the Si_3N_4 sphere array. We confirmed that this oscillating wave form continues more than 300 ps after the main peak at 25 ps. On the other hand, Fig. 1(c) shows that the remarkable oscillating wave form is not observed in the THz wave transmitted through the PTFE sphere array. We also measured the THz wave forms transmitted through a 3.95-mm-thick Si_3N_4 plate and a 3.1-mm-thick PTFE plate for comparison and observed that the oscillating wave form does not appear in the THz wave forms transmitted through these plates. This fact indicates that the oscillating wave form is caused by both the structural shape of the sphere array and the large refractive index of the material. The oscillating wave form for the Si_3N_4 sphere-array photonic crystal is due to the slow leakage of the electromagnetic energy from the photonic band modes resonantly excited by the incident wave.[17] The above results indicate that the confinement of the electromagnetic energy in the sphere and its leakage as a transmitted electromagnetic wave are considerably affected by the refractive index of the spheres.

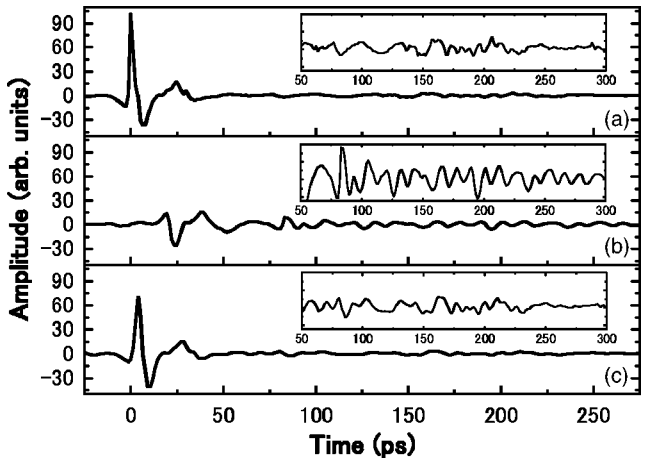

FIG. 1. (a) Time domain THz wave forms of the incident wave and those transmitted through (b) Si_3N_4 and (c) PTFE sphere arrays at normal incidence. The insets show the enlarged wave forms in the time range from 50 to 300 ps.

The above discussion is clearly supported by the power transmission spectra deduced by Fourier transformation of the THz wave forms. Figure 2 shows the measured and calculated power transmission spectra at normal incidence. For normal incidence, first-order Bragg diffraction occurs at 109.1 GHz. For calculating the transmission spectra, the effect of the transmission spectra of the thin vinyl films on the photonic crystal is taken into account.[8] The calculation of the transmission spectra is based on the vector KKR method using the complex refractive index with the dispersion of the material. All the theoretical data presented throughout the paper are calculated using the vector KKR formalism.[1,16] Figure 2 indicates that good agreement between the experiment and the calculation for the transmittance has been obtained in a wide frequency range. The photonic bands of the 2D sphere-array photonic crystals show up mostly as dips in the transmission spectra.[7] Figure 2(a) shows that many dis-

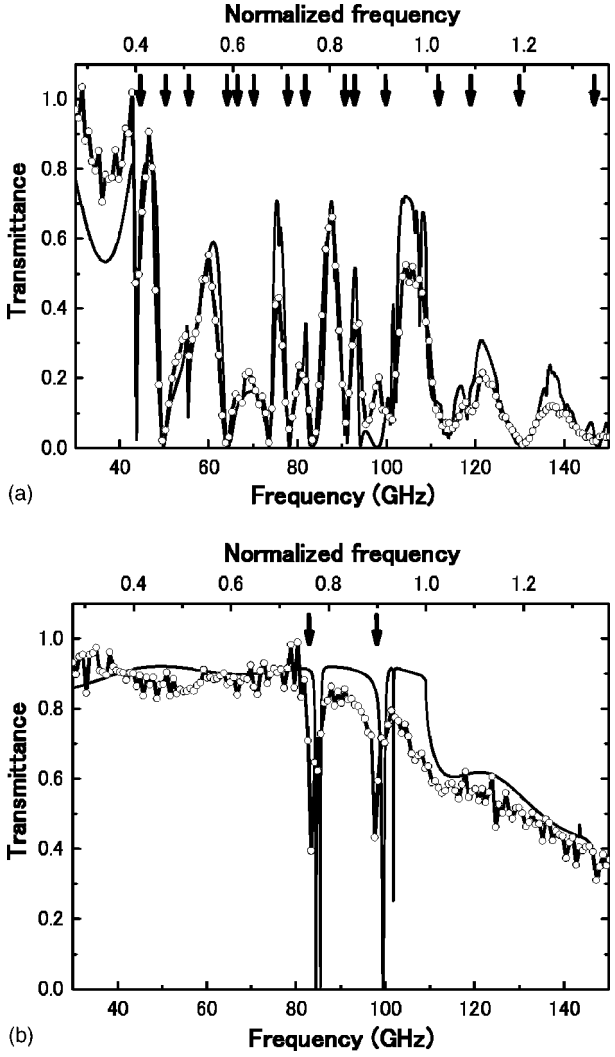

FIG. 2. Power transmission spectra of (a) the Si_3N_4 sphere array and (b) the PTFE sphere array for normal incidence. Circles with solid lines and the thin lines represent data obtained by the THz TDS and the calculation based on the vector KKR method, respectively. Arrows show the dip frequency positions in the experimental results. The normalized frequency is $\omega a\sqrt{3}/4\pi c$, where a is the lattice constant and c is the velocity of light in vacuum.

tinct dips are observed in the transmission spectrum of the Si_3N_4 sphere array owing to the excitation of optically active photonic band modes that couple to a plane-wave mode existing in the outer world. On the other hand, in the experimental transmission spectrum of the PTFE sphere array, only two major distinct sharp dips are observed. The calculated transmission spectrum of the PTFE sphere array shows four distinct sharp dips at 84.44, 85.43, 99.52, and 101.77 GHz. Since the frequency resolution of the present measurement system is estimated to be 0.75 GHz, these dips cannot be resolved completely in the experimental spectrum. Such a low population of the modes will help us to identify the origin of the fine structures appeared in the optical response. It is also interesting that the photonic crystal with small refractive index contrast between PTFE ($n \sim 1.44$) and air ($n = 1.00$) can produce a mode with a very high Q value corresponding to the fine structure seen at 101.77 GHz in Fig. 2(b), for example. By comparing Figs. 2(a) and 2(b), it is strongly expected that the population of the modes excited by the incident electromagnetic wave decreases with decreasing refractive index of the material in addition to the blueshift of the mode frequencies.

For understanding the origin of these modes, we calculated (a) the spectra of the ODOS of the gallery modes for an isolated dielectric sphere from the viewpoint of the tight-binding treatment[7,18] and (b) the photonic band structure based on the guided wave mode in the dielectric slab (empty lattice approximation).[17,19] In the former calculation, the whispering gallery mode localized at an isolated sphere is considered. In the sphere array, the incident electromagnetic wave undergoes a sequential Mie scattering by individual spheres. Since the photonic band structure of the dielectric sphere array is constructed by the interaction of the gallery modes between adjacent spheres, the characteristics of the gallery modes are expected to appear in the photonic band structure. In the latter calculation, the 2D dielectric sphere array is regarded approximately as a dielectric slab with periodic hollows on the surfaces. In this case, the photonic band structure is considered as the folding up of the guided wave modes in the slab. The calculation of the guided wave mode was done under the following assumptions: (i) the thickness of the slab is equal to the diameter of the sphere, and (ii) the refractive index of the slab n' is real, without dispersion, and taken as the spatially averaged value of the refractive index for the sphere array n.

The left-hand side figures of Fig. 3 show the experimental (open circles) and theoretical (closed circles) photonic band structures for the p-polarization-active modes determined by the dip positions in the transmission spectra. The dispersion relations of the 2D photonic band in the experiment are obtained from the incidence angle dependence of the transmittance.[7,8] The calculated results were obtained using the experimentally obtained complex refractive index of the material. These results demonstrate a good agreement between the experimental and theoretical photonic band structures. It is clearly seen that the photonic band structure of the Si_3N_4 sphere array has some photonic bands with small dispersions around 44, 56, and 68 GHz. Since small dispersive photonic bands indicate strong optical confinement, the large magnitude of the ODOS is realized in those photonic bands.[7,18]

The photonic band structure (left-hand side) is compared with the ODOS calculated for the localized gallery mode (right-hand side) as shown in Fig. 3. In Fig. 3, l represents the angular momentum, and M and N represent two vector spherical waves in the usual way.[20] In this calculation of the ODOS, the refractive index is assumed to be real. Figure 3(a) shows that some of the photonic bands of the Si_3N_4 sphere array are correlated with the gallery modes in an isolated Si_3N_4 sphere. In particular, the small dispersive photonic bands around 44, 56, and 68 correspond to the gallery modes with $l=2$, 3, and 4 of the M wave, respectively. This good correspondence means that the characteristics of the gallery mode for an isolated Si_3N_4 sphere indeed appear in the photonic band structure of the Si_3N_4 sphere array.[7] Here it is important to note that the width of the peaks in the ODOS represents the lifetime broadening, being comparable with

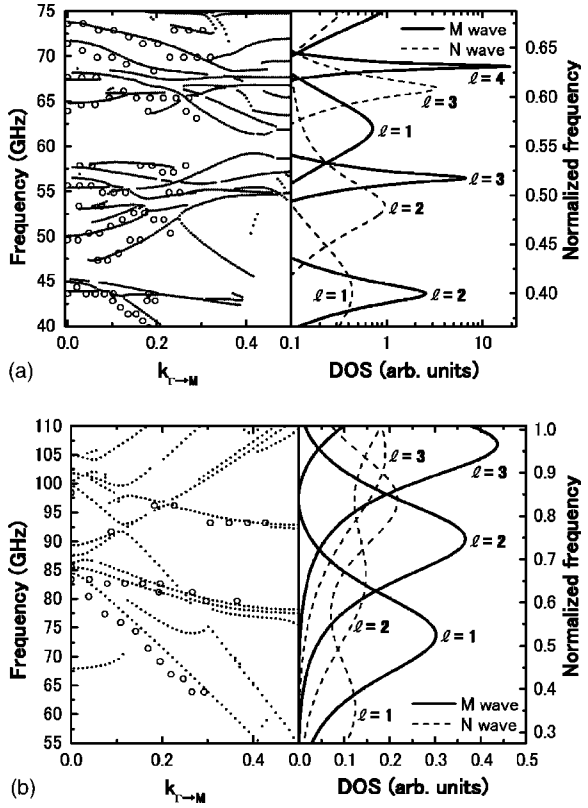

FIG. 3. Photonic band structures corresponding to the *p*-polarized wave (left-hand side) and the ODOS of an isolated sphere (right-hand side) for (a) Si_3N_4 and (b) PTFE. Open and closed circles represent the dip positions in the transmission spectra of the experimental data and theoretical calculation, respectively. The horizontal axis is normalized so that $k_{\Gamma\to M}=0.5$ at the *M* point of the first Brillouin zone.

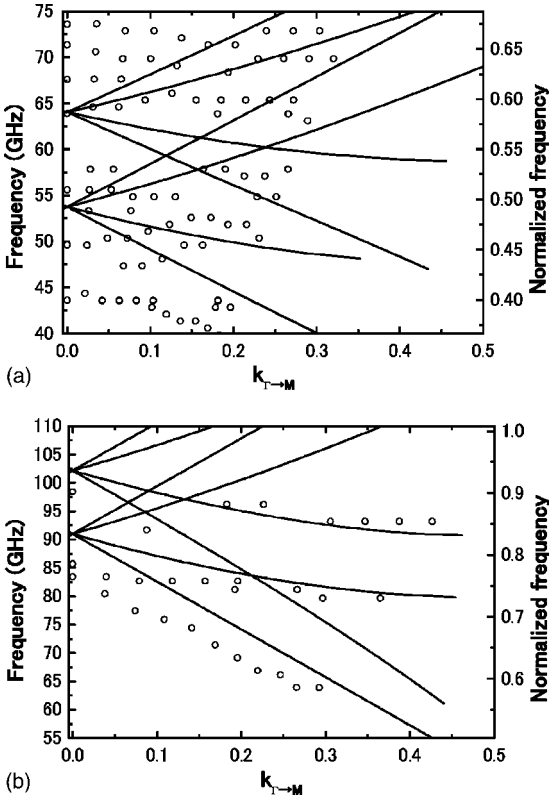

FIG. 4. Experimental (open circles) and calculated (solid lines) photonic band structures corresponding to the *p*-polarized wave for (a) Si_3N_4 and (b) PTFE sphere arrays. The calculation is based on the guided wave mode in a slab (see text). In this calculation, the refractive index of the material, *n*, for Si_3N_4 and PTFE is taken as 2.99 and 1.44, respectively.

the width of the photonic band. We can also confirm that the $(2l+1)$-fold degeneracy of the Mie resonance of an isolated sphere partly lifts. Thus, this conclusion suggests that the tight-binding picture based on sphere resonances holds well in the sphere-array photonic crystal with a large refractive index. On the other hand, the photonic bands of the PTFE sphere array do not seem to be strongly correlated with the gallery mode as shown in Fig. 3(b). The larger width of the peaks in the ODOS prevents us from applying the tight-binding picture to this case. Since the confinement of the gallery modes of an isolated PTFE sphere is weak owing to the small difference of refractive indices between PTFE and air, corresponding to a weak attractive potential for the electromagnetic wave, the characteristics of the gallery mode are not evident in the photonic band structure.

Next, we compared the experimental photonic band structure (open circles) with the photonic band structure of *p*-polarization-active modes calculated based on the TM guided wave mode (solid lines) as shown in Fig. 4. Note that TM modes in a slab correspond to *p*-polarization-active modes in a 2D sphere-array photonic crystal. It is important to emphasize that a guided wave mode above the light line turns into a radiation mode in the empty lattice treatment. In the Si_3N_4 sphere-array case, most of the experimental photonic bands do not seem to be correlated with the dispersion curves calculated based on the guided wave mode. On the other hand, Fig. 4(b) shows that the experimental photonic band structure of the PTFE sphere array is reproduced by the photonic band structure originated in the guided wave mode. This result suggests that the sphere-array photonic crystal with small refractive index contrast can be regarded as a slab with weak modulation of the refractive index, in spite of the peculiar shape of spheres in the unit cell. We conjecture that the crossover from the guided-wave-like to the localized-gallery-mode-like characteristics in the optical properties of sphere-array photonic crystals occurs with increasing refractive index of the materials.

To confirm this conjecture, the *p*-polarization-active photonic band structures were calculated for a 2D sphere-array photonic crystal with various refractive indices of the material *n* as shown in Fig. 5. Open circles and solid lines represent the calculated dip positions in the transmission spectra of the 2D sphere array and the calculated photonic band structures based on the TM guided wave mode in the corresponding dielectric slab, respectively. Figure 5(a) indicates that the photonic band structure of a sphere-array photonic crystal with a small relative dielectric constant $\epsilon(=n^2)$ is reproduced well by the guided wave mode. With increasing relative dielectric constant, the agreement becomes worse [Fig. 5(b)] and the apparent agreement almost disappears in the case of $\epsilon=4$ [Fig. 5(c)]. In Fig. 5(c), a group of relatively

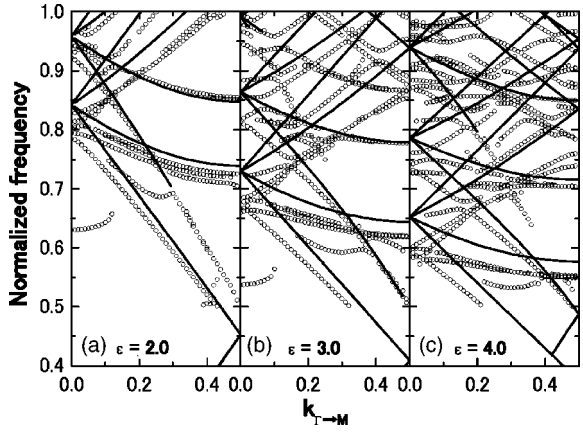

FIG. 5. Refractive index dependence of calculated photonic band structures. Open circles and solid lines represent the dip positions in the transmission spectra of a 2D triangular lattice of spheres ($a=d$) and the guided wave mode in a dielectric slab, respectively. ϵ represents the relative dielectric constant of material for the sphere.

small dispersive photonic bands appears around the normalized frequency of 0.86. We confirmed that this photonic band group corresponds well to the gallery mode with $l=3$ of the M wave. In Fig. 6, the transmission spectra for normal incidence of the sphere-array photonic crystals are plotted for various values of the relative dielectric constant. The spectrum changes from the guided resonance type for a photonic crystal slab with sharp dips[17,21,22] for $\epsilon=1.5$ and 2.1 to complicated structures reflecting the gallery modes for over $\epsilon=5$ in addition to the redshift of the mode frequencies. Accordingly, the crossover from the guided-wave nature to the localized-whispering-gallery-mode nature occurs around the relative dielectric constant of $\epsilon=3$. In the study of the sphere-array photonic crystals, silica, polystyrene, polymethylmethacrylate (PMMA), etc. are often used as the material in the visible range.[23–25] Since the refractive indices of these materials are similar to the case of Fig. 5(a), the optical properties of a sphere-array photonic crystal made of those materials can be understood by simple guided wave modes.

IV. CONCLUSION

We have investigated the refractive index dependence of the transmission properties for a 2D dielectric-sphere-array photonic crystal. Arrays of Si_3N_4 ($n\sim2.99$) and PTFE ($n\sim1.44$) spheres with the same size were prepared in the same triangular lattice structure. The results indicate that the characteristics of the gallery mode for an isolated dielectric sphere appear in the photonic band structure of the sphere array with a large refractive index, whereas the characteristics of the guided wave mode in a dielectric slab appear dominantly in the photonic band structure of the sphere array with a small refractive index. The crossover from the guided

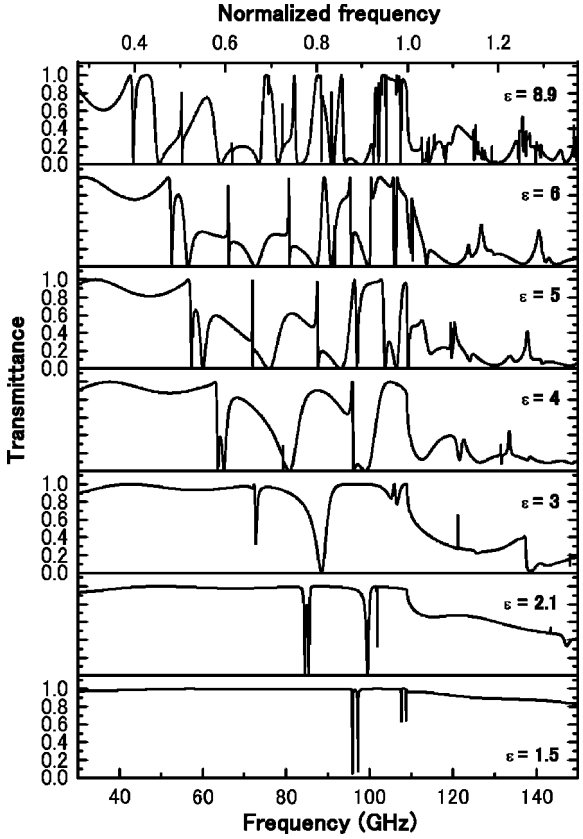

FIG. 6. The relative dielectric constant dependence of the calculated power transmission spectra of the 2D dielectric-sphere-array photonic crystal at normal incidence. The structure of the photonic crystal is assumed to be a 2D triangular lattice of dielectric spherical balls with $d=a=3.175$ mm. The first diffraction occurs at 109.1 GHz. The imaginary part of the dielectric constant of the material is neglected in this calculation. The relative dielectric constants of 2.1 and 8.9 are similar to the PTFE and Si_3N_4 cases, respectively.

wave to the localized gallery mode nature in the optical properties of sphere-array photonic crystals occurs with increasing refractive index of the materials. The photonic band structure based on the guided wave mode in a dielectric slab can be used to interpret the optical properties of the dielectric-sphere-array photonic crystal made of materials with small refractive index ($\epsilon\lesssim3$).

ACKNOWLEDGMENTS

We thank Dr. T. Nagashima and Professor M. Tani for fruitful discussions, and Dr. S. Yano for sample preparation. This work is supported by a Grant-in-Aid for Scientific Research from the Ministry of Education, Culture, Sports, Science and Technology of Japan. T.K. acknowledges financial support from JSPS Research Grants for Young Scientists.

*Electronic address: kondo@iis.u-tokyo.ac.jp
†Present address: Institute of Physics, University of Tsukuba, 1-1-1 Tennoudai, Tsukuba 305-8571, Japan.

[1] K. Ohtaka, Phys. Rev. B **19**, 5057 (1979).
[2] E. Yablonovitch, Phys. Rev. Lett. **58**, 2059 (1987).
[3] *Photonic Crystals—Physics, Fabrication and Applications*, edited by K. Inoue and K. Ohtaka (Springer, Berlin, 2004).
[4] R. Colombelli, K. Srinivasan, M. Troccoli, O. Painter, C. F. Gmachl, D. M. Tennant, A. M. Sergent, D. L. Sivco, A. Y. Cho, and F. Capasso, Science **302**, 1374 (2003).
[5] S. Noda, A. Chutinan, and M. Imada, Nature (London) **407**, 608 (2000).
[6] Y. Akahane, T. Asano, B.-H. Song, and S. Noda, Nature (London) **425**, 944 (2003).
[7] K. Ohtaka, Y. Suda, S. Nagano, T. Ueta, A. Imada, T. Koda, J. S. Bae, K. Mizuno, S. Yano, and Y. Segawa, Phys. Rev. B **61**, 5267 (2000).
[8] T. Kondo, M. Hangyo, S. Yamaguchi, S. Yano, Y. Segawa, and K. Ohtaka, Phys. Rev. B **66**, 033111 (2002).
[9] S. Yamaguti, J. Inoue, O. Haeberlé, and K. Ohtaka, Phys. Rev. B **66**, 195202 (2002).
[10] K. Yamamoto, R. Sakakibara, S. Yano, Y. Segawa, Y. Shibata, K. Ishi, T. Ohsaka, T. Hara, Y. Kondo, H. Miyazaki, F. Hinode, T. Matsuyama, S. Yamaguti, and K. Ohtaka, Phys. Rev. E **69**, 045601 (2004).
[11] W. M. Robertson, G. Arjavalingam, R. D. Meade, K. D. Brommer, A. M. Rappe, and J. D. Joannopoulos, Phys. Rev. Lett. **68**, 2023 (1992).
[12] F. Miyamaru, T. Kondo, T. Nagashima, and M. Hangyo, Appl. Phys. Lett. **82**, 2568 (2003).
[13] A. Chelnokov, S. Rowson, J.-M. Lourtioz, L. Duvillaret, and J.-L. Coutaz, Electron. Lett. **33**, 1981 (1997).
[14] M. van Exter and D. Grischkowsky, Phys. Rev. B **41**, 12 140 (1990).
[15] M. Hangyo, T. Nagashima, and S. Nashima, Meas. Sci. Technol. **13**, 1727 (2002).
[16] N. Stefanou, V. Karathanos, and A. Modinos, J. Phys.: Condens. Matter **4**, 7389 (1992).
[17] S. Fan and J. D. Joannopoulos, Phys. Rev. B **65**, 235112 (2002).
[18] E. Lidorikis, M. M. Sigalas, E. N. Economou, and C. M. Soukoulis, Phys. Rev. Lett. **81**, 1405 (1998).
[19] K. Sakoda, *Optical Properties of Photonic Crystals* (Springer, Berlin, 2001), Chap. 8.
[20] J. A. Stratton, *Electromagnetic Theory* (McGraw-Hill, New York, 1941) p. 397.
[21] V. N. Astratov, I. S. Culshaw, R. M. Stevenson, S. M. Whittaker, M. S. Skolnick, T. F. Krauss, and D. M. De La Rue, J. Lightwave Technol. **17**, 2050 (1999).
[22] F. Miyamaru, T. Kondo, T. Nagashima, and M. Hangyo, IEEJ Trans. FM **123**, 995 (2003) (in Japanese).
[23] Y. A. Vlasov, X.-Z. Bo, J. C. Sturm, and D. J. Norris, Nature (London) **414**, 289 (2001).
[24] H. Guo, H. Chen, P. Ni, Q. Zhang, B. Cheng, and D. Zhang, Appl. Phys. Lett. **82**, 373 (2003).
[25] P. Ferrand, M. Egen, R. Zentel, J. Seekamp, S. G. Romanov, and C. M. Sotomayor Torres, Appl. Phys. Lett. **83**, 5289 (2003).